

# Label-free optical biosensing using a horizontal air-slot SiN<sub>x</sub> microdisk resonator

Shinyoung Lee,<sup>1</sup> Seok Chan Eom,<sup>1</sup> Jee Soo Chang,<sup>1</sup> Chul Huh,<sup>3</sup> Gun Yong Sung,<sup>3</sup> and Jung H. Shin<sup>1,2</sup>

<sup>1</sup>Department of Physics, KAIST 373-1 Guseong-dong, Yuseong-Gu, Daejeon, Korea

<sup>2</sup>Graduate School of Nanoscience and Technology (WCU), KAIST 373-1 Guseong-dong, Yuseong-Gu, Daejeon, Korea

<sup>3</sup>Biosensor Research Team, ETRI, Daejeon 305-700, Korea  
[jhs@kaist.ac.kr](mailto:jhs@kaist.ac.kr)

**Abstract:** We demonstrate label-free optical biosensing using a horizontal air-slotted silicon-rich silicon nitride (SiN<sub>x</sub>) microdisk resonator. Due to the strong confinement of light in the air-slot, a large resonance shift of 6.2 nm is observed upon reaction of the biotin-functionalized disk with a streptavidin solution with concentration of 2.5 μg/ml. Assuming a linear relationship between resonance shift and streptavidin concentration, we estimate the sensitivity to be  $2.5 \pm 0.2$  nm/(μg/ml). Comparing this value with surface sensitivity of 5.7 nm/nm calculated using FDTD simulations, a detection limit of  $30 \pm 2$  ng/ml, is extrapolated.

©2010 Optical Society of America

OCIS codes: (230.5750) Resonators; (280.1415) Biological sensing and sensors.

---

## References and links

1. X. Fan, I. M. White, S. I. Shopova, H. Zhu, J. D. Suter, and Y. Sun, "Sensitive optical biosensors for unlabeled targets: a review," *Anal. Chim. Acta* **620**(1-2), 8–26 (2008).
2. A. Densmore, M. Vachon, D. X. Xu, S. Janz, R. Ma, Y. H. Li, G. Lopinski, A. Delâge, J. Lapointe, C. C. Luebbert, Q. Y. Liu, P. Cheben, and J. H. Schmid, "Silicon photonic wire biosensor array for multiplexed real-time and label-free molecular detection," *Opt. Lett.* **34**(23), 3598–3600 (2009).
3. K. De Vos, I. Bartolozzi, E. Schacht, P. Bienstman, and R. Baets, "Silicon-on-Insulator microring resonator for sensitive and label-free biosensing," *Opt. Express* **15**(12), 7610–7615 (2007).
4. V. R. Almeida, Q. Xu, C. A. Barrios, and M. Lipson, "Guiding and confining light in void nanostructure," *Opt. Lett.* **29**(11), 1209–1211 (2004).
5. G. S. Wiederhecker, C. M. B. Cordeiro, F. Couny, F. Benabid, S. A. Maier, J. C. Knight, C. H. B. Cruz, and H. L. Fragnito, "Field enhancement within an optical fibre with a subwavelength air core," *Nat. Photonics* **1**(2), 115–118 (2007).
6. J. T. Robinson, L. Chen, and M. Lipson, "On-chip gas detection in silicon optical microcavities," *Opt. Express* **16**(6), 4296–4301 (2008).
7. C. A. Barrios, K. B. Gylfason, B. Sánchez, A. Griol, H. Sohlström, M. Holgado, and R. Casquel, "Slot-waveguide biochemical sensor," *Opt. Lett.* **32**(21), 3080–3082 (2007).
8. C. A. Barrios, M. J. Bañuls, V. González-Pedro, K. B. Gylfason, B. Sánchez, A. Griol, A. Maquieira, H. Sohlström, M. Holgado, and R. Casquel, "Label-free optical biosensing with slot-waveguides," *Opt. Lett.* **33**(7), 708–710 (2008).
9. T. Claes, J. G. Molera, K. De Vos, E. Schacht, R. Baets, and P. Bienstman, "Label-Free Biosensing With a Slot-Waveguide-Based Ring Resonator in Silicon on Insulator," *IEEE Photo. J.* **1**(3), 197–204 (2009).
10. S. Lee, S. C. Eom, J. S. Chang, C. Huh, G. Y. Sung, and J. H. Shin, "A silicon nitride microdisk resonator with a 40-nm-thin horizontal air slot," *Opt. Express* **18**(11), 11209–11215 (2010).
11. L. Xianghuai, Y. Yuehui, Z. Zhihong, H. Wei, Z. Shichang, J. Zuqing, C. Ming, X. Shoulian, S. Taniguchi, T. Shibata, and K. Nakamura, "Properties and structure of silicon nitride films synthesized by ion-beam-enhanced deposition," *Surf. Coat. Tech.* **46**(2), 227–232 (1991).
12. J. T. Robinson, K. Preston, O. Painter, and M. Lipson, "First-principle derivation of gain in high-index-contrast waveguides," *Opt. Express* **16**(21), 16659–16669 (2008).
13. I. M. White, and X. Fan, "On the performance quantification of resonant refractive index sensors," *Opt. Express* **16**(2), 1020–1028 (2008).

14. K. M. De Vos, I. Bartolozzi, P. Bienstman, R. Baets, and E. Schacht, "Optical biosensor based on silicon-on-insulator microring cavities for specific protein binding detection," in *Nanoscale Imaging, Spectroscopy, Sensing, and Actuation for Biomedical Applications IV*(SPIE, San Jose, CA, USA, 2007), pp. 64470K–64478.
15. N. Daldosso, M. Melchiorri, F. Riboli, M. Girardini, G. Pucker, M. Crivellari, P. Bellutti, A. Lui, and L. Pavesi, "Comparison Among Various Si<sub>3</sub>N<sub>4</sub> Waveguide Geometries Grown Within a CMOS Fabrication Pilot Line," *J. Lightwave Technol.* **22**(7), 1734–1740 (2004).
16. J. S. Chang, S. C. Eom, G. Y. Sung, and J. H. Shin, "On-chip, planar integration of Er doped silicon-rich silicon nitride microdisk with SU-8 waveguide with sub-micron gap control," *Opt. Express* **17**(25), 22918–22924 (2009).
17. I. Fränz, and W. Langheinrich, "Conversion of silicon nitride into silicon dioxide through the influence of oxygen," *Solid-State Electron.* **14**(6), 499–505 (1971).
18. A. V. Pesse, G. R. Warrier, and V. K. Dhir, "An experimental study of the gas entrapment process in closed-end microchannels," *Int. J. Heat Mass Transfer* **48**(25-26), 5150–5165 (2005).
19. D. Hohfeld, and H. Zappe, "An all-dielectric tunable optical filter based on the thermo-optic effect," *J. Opt. A, Pure Appl. Opt.* **6**(6), 504–511 (2004).

---

## 1. Introduction

With the development of microphotonic technology, great strides have been made in developing compact and highly sensitive optical biosensors on a chip [1]. Typically, label-free optical biosensors sense biomaterials by detecting the change in the effective refractive index of itself or its surroundings. In the widely used configuration, the light used for sensing is guided within the sensor by total internal reflection due to refractive index contrast. Unfortunately, this can result in small overlap between the optical mode and the sensing material, since much of the optical mode is confined within the sensor itself, and changes in the surrounding analyte are sensed via evanescent field. As a consequence, the devices tend to require either long interaction distance [2] or a high Q factor to obtain sufficient sensing efficiency [3].

Recently, a slot-waveguide structure that consists of a thin, low-index "slot" fabricated in a high-index waveguide has attracted a great attention [4]. Similar to a holey optical fiber [5], this opens up the interior region of the waveguide, where the electric field intensity is highest, available for sensing. Furthermore, the requirement that dielectric displacement be continuous results in strong concentration of electric field right on the inside surface of the slot, where a biomaterial to be sensed would be adsorbed. This has led research into to application of slot-waveguide structure for optical biosensor that can overcome the possible limitations of evanescent field sensing. By now, sensors based on resonators that employ the slot-structure to enhance the interaction between photons and materials in the slot region have been reported [6–9].

So far, most research into slot-structure based optical biosensors used a vertical slot structure which consists of a thin, vertical slot etched in the center of a high-index waveguide that forms a resonator. Etching such thin, high aspect ratio slot, however, is difficult, and usually requires expensive lithography techniques such as e-beam or deep-UV. Furthermore, etching such a vertical slot can result in roughness on the slot surface, right where the E-field intensity is the highest, and can lead to subsequent degradation in the Q-factor and the limit of detection.

We have previously reported that such problems can be overcome by using a horizontal air-slotted SiN<sub>x</sub> microdisk resonator fabricated by multilayer deposition and selective etching. In this case, as the slot is defined through deposition, ultra-thin slots with extremely smooth slot walls can easily be fabricated using conventional, micron-scale photolithography only [10]. In this paper, we report on using such SiN<sub>x</sub> disk resonators with a 40-nm thin, horizontal air-slot for bio-sensing applications. We find that the resonators are quite robust such that the 40-nm thin air slot is preserved throughout the fabrication and measurement processes that involve repeated washing/drying steps and wide variations in temperature and pH. We observe a resonance peak shift of 6.2 nm upon reaction of the biotin-functionalized disk with a streptavidin solution with concentration of 2.5 μg/ml, with a saturation value of more than 9 nm. Assuming a linear relationship between resonance shift and streptavidin concentration,

we estimate the sensitivity to be  $2.5 \pm 0.2$  nm/( $\mu\text{g/ml}$ ). Comparing this value with results of FDTD simulations, we calculate the surface sensitivity and the limit of detection to be 5.7 nm/nm and  $30 \pm 2$  ng/ml, respectively.

## 2. Experimental

A 240nm-thin  $\text{SiN}_x$ / 40nm-thin  $\text{SiO}_2$ / 240nm-thin  $\text{SiN}_x$  multilayer thin film was deposited on a silicon substrate using reactive ion beam sputter deposition method. After deposition, the film was annealed at  $800^\circ\text{C}$  for 30 min in Ar environment to densify the film. The refractive index of  $\text{SiN}_x$  layer after annealing was obtained to be 2.308 by ellipsometry (data not shown) in the 1500nm region. We note that this is much higher than the value of  $\sim 2.0$  reported for refractive index of  $\text{Si}_3\text{N}_4$  [11] due to the excess Si content of the deposited layers, and will result in stronger slot effect. Furthermore, using such  $\text{SiN}_x$  thin films for resonator fabrication also give us the advantages of lower cost, higher stiffness, and transparency in the visible region for possible operation in aqueous environment over SOI [13].  $15\mu\text{m}$  diameter microdisks were then patterned with photolithography and dry etching. 30% KOH solution was then used to selectively undercut the multilayer film to fabricate pedestal-type microdisk resonators. Finally, a buffered hydrofluoric acid etch followed by a simple air drying was used to selectively etch the  $\text{SiO}_2$  layer and define a  $\sim 2$   $\mu\text{m}$  deep horizontal air slot. In the previous report, we have shown that such a depth is sufficient to eliminate the effect of the central  $\text{SiO}_2$  spacer on the fundamental mode [10].

The surfaces of the fabricated slot disks were functionalized by following process. First, the sample was cleaned and oxidized by immersing in solutions of 5:1:1  $\text{H}_2\text{O}:\text{H}_2\text{O}_2:\text{HN}_3-\text{H}_2\text{O}$  and then 4:1:1  $\text{H}_2\text{O}:\text{H}_2\text{O}_2:\text{HCl}$  at  $80^\circ\text{C}$  for 10 min each in order to expose hydroxyl group (-OH) on the surface of  $\text{SiN}_x$ . Afterwards, amine group ( $-\text{NH}_2$ ) was formed by immersing the samples in 5% solution of 3-aminoprophltriethoxysilane (APTES) in dry ethanol for 2 hours at room temperature. After rinsing with ethanol and distilled water, the surface was still hydrophilic which indicates hydrophilic amino end-groups [14]. The sample was dried with  $\text{N}_2$  gas and annealed on the hotplate of  $\sim 100^\circ\text{C}$  for 20 min to stabilize the amino group. After silanization, the sample was dipped in NHS-biotin (Pierce) in dimethyl sulfoxide (DMSO) during 15 hours at room temperature and cleaned with distilled water. Afterward, the samples were allowed to react with 500 $\mu\text{l}$  of fluorescein (FITC) conjugated streptavidin (Peirce) in PBS (pH 7.3) with concentration of 1.25, 2.5, 5, 10, 20  $\mu\text{g/ml}$  for 1 hour and then rinsed with water.

The images of the slot-sensor during the various stages of its fabrication and usage are shown in Fig. 1. We observe successful fabrication of the air-slot disk resonator. More importantly, Fig. 1 demonstrates that the 40-nm thin air-slot structure is preserved throughout the fabrication process despite repeated washing/drying steps and wide variations in temperature and pH, and repeated measurements over long period of time in the ambient air.

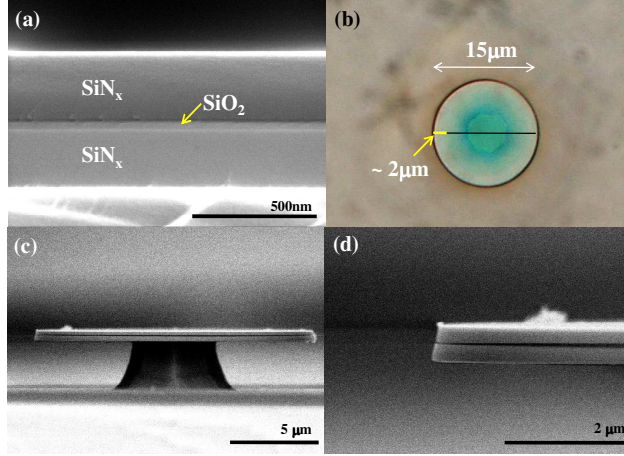


Fig. 1. (a) SEM image of the deposited multilayer thin film prior to disk formation, (b) DIC optical microscope image of the fabricated microdisk after air slot fabrication. The green inner boundary indicates the silicon post and the whiter outer region indicates air slot with depth of more than 2μm. (c)(d) SEM images of fabricated slot disk after whole sensing process. Note that the air-slot is maintained despite repeated washing/drying measurement steps.

### 3. Results and Discussion

Based on the fabricated structure shown in Fig. 1, the sensing efficiency of the air-slot microdisk resonator was calculated using finite difference time domain (FDTD) method. The edge of the disk was set to be 10° sloped based on the SEM image. The grid size of vertical direction was 2 nm and a single fundamental TM-like mode was excited using a single Gaussian point source. Figure 2(a) shows the calculated mode profile, demonstrating the highly concentrated  $|E|^2$  in the air slot region. The confinement factor is defined as [12]

$$\Gamma = \frac{n_A c \varepsilon_0 \iint_A |E|^2 dx dy}{\iint_{\infty} \text{Re}\{\mathbf{E} \times \mathbf{H}^*\} \cdot \hat{e}_z dx dy} \equiv \frac{n_g}{n_A} \gamma_A, \text{ where } \gamma_A = \frac{\iint_A \varepsilon |E|^2 dx dy}{\iint_{\infty} \varepsilon |E|^2 dx dy}. \quad (1)$$

Here  $c$  is the speed of light in vacuum,  $n_g$  is the group index and  $n_A$  is the refractive index in the region  $A$ . The  $\gamma_A$  term represents the spatial confinement factor. Based on the simulated mode profile, the shift in the position of the resonance peak of the resonator due to adsorption of a thin layer with a refractive index of 1.45 typical for a dried biofilm is calculated. For a configuration described schematically in Fig. 2 (b), the resonance position shifts linearly with layer thickness, as is shown in Fig. 2 (c). The surface sensitivity of the resonator,  $S_{\text{surface}}$  defined as

$$S_{\text{surface}} = \partial \lambda_{\text{res}} / \partial t_{\text{bio}} [nm / nm], \quad (2)$$

is found to be 5.73 nm/nm for the mode number of  $m = 45$ . It should be noted here that the high  $S_{\text{surface}}$  value is mostly due to the adsorption of biofilm on the inside surface of the slot. For example, give a 5 nm thick adsorbed film, the spatial confinement factor ( $\gamma_A$ ) with the film is calculated to be 6.3%. Of this, the spatial confinement factor with the film adsorbed on the inside surface is calculated to be 5.4%, which corresponds to 85% of the total sensitivity. In contrast, the surface sensitivity with the film adsorbed on the top of the upper disk and the bottom of the lower disk is calculated to be 0.80 nm/nm only, confirming the importance of the slot-structure for achieving the high sensitivity.

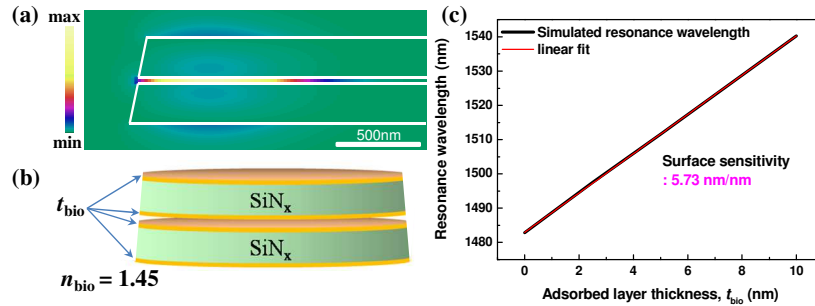


Fig. 2. (a) Simulated mode profile of IEF with bare fabricated structure (b) schematic of surface sensing (c) Calculated shift in the resonance wavelength versus thickness of adsorbed layer with a refractive index of 1.45. The surface sensitivity is obtained as 5.73nm/nm with linear fit.

The actual surface sensing capability of fabricated air slot resonators was measured using tapered fiber coupling. Figure 3 shows the schematic diagram of measurement setup. A tunable laser which spans from 1470nm to 1545 nm was used as the light source, and a tapered fiber with a diameter of  $\sim 1\mu\text{m}$  was used to evanescently couple light into and out of the resonator. The input polarization was controlled with a fiber polarization controller to TM-like mode in order to excite the slot-modes of the resonator. The fiber position was controlled not to touch the disk in order to reduce the scattering loss and unwanted peak shift due to contact between the resonator and the fiber.

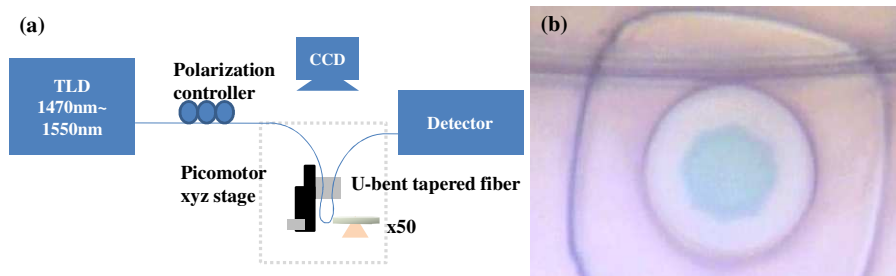


Fig. 3. (a) Schematic of the measurement system. (b) CCD image of a slot disk coupled with a tapered fiber. The fiber diameter is  $\sim 1\mu\text{m}$ .

The measured transmission spectra from the same disk before and after biotin-streptavidin reaction in a streptavidin solution with a concentration of  $20\mu\text{g/ml}$  are shown in Fig. 4(a). We observe two sets of strong resonance dips, one with FSR of 22.9 and the other with 23.6, as indicated. Based on the calculated FSR of 23.3nm and 24.7 nm for the fundamental and 1st high order radial modes, respectively, we identify the peaks as the fundamental and first-order radial mode resonance dips, respectively. We find that we observe the same sets of two dips, with FSR of 22.9 and 23.7 nm, even after the streptavidin binding. We find, however, that the resonance dips corresponding to the fundamental radial modes have shifted by more than 9 nm upon streptavidin binding, while those corresponding to the first order radial modes have shifted by about 4 nm only. This is consistent with their identification, as the first order higher radial mode is expected to have lower sensitivity due to its optical mode being deeper into the slot, where adsorption efficiency of bio materials is expected to be lower due to capillary filling effect [18]. Based on the calculated sensitivity of 5.73 nm/nm as shown in Fig. 2, we estimate the average streptavidin layer thickness to be  $1.7 \pm 0.1$  nm.

For comparison, an oxidized Si wafer was processed using the same surface-functionalized protocol using the same  $20\mu\text{g/ml}$  streptavidin solution. The average thickness of the resulting streptavidin film was estimated using ellipsometry and assuming a refractive index of 1.45 to be  $\sim 2.2$  nm. Considering the fully oxidized surface of the oxide wafer [16]

and planar structure [17], this value agrees reasonably well with the above value of  $1.7 \pm 0.1$  nm, and further validates the identification of the resonance dips.

Based on this identification, the concentration-dependence of resonance dip shift of the fundamental radial mode is investigated, as is shown in Fig. 4(b). The data points show the average peak shifts of three different disks ( $N = 3$ ). The error bars indicate the standard deviation of observed values, possibly due to fabrication errors. Assuming a linear relationship between resonance peak shift and the streptavidin concentration at low streptavidin concentrations, the sensitivity of the slot disk resonator is estimated to be  $2.5 \pm 0.2$  nm/( $\mu\text{g/ml}$ ). We also find that the resonance shifts saturates at 9.7 nm above a streptavidin concentration of 5  $\mu\text{g/ml}$ , in agreement with previous reports [3], which we attribute to saturation of streptavidin binding sites on the disk surfaces [3].

Interestingly, as can be seen in Fig. 4(c) that shows fine scan measurements of resonance dips, the Q-factor of the resonator does not change upon streptavidin binding, remaining near  $\sim 7,000$ . This demonstrates the robustness of the air-slot structure to resist process-related structural damages. Still, the Q-factor of 7,000 corresponds to optical loss of  $\sim 20$  dB/cm, which is rather high, and should be improved for better sensor performance. We note, however, that absorption loss of SiN waveguides has been reported to be as low as  $0.1 \pm 0.05$  dB/cm even at 780 nm [15]. Furthermore, the radiation-loss limited Q-factor of slot-disk resonator can be as high as  $10^7$ , while the slot-surfaces are ultra-smooth with RMS roughness of 0.51 nm only [10]. On the other hand, we have reported recently that in similarly prepared SiN disk resonators, Q-factors are dominated by scattering by process-related sidewall roughness [16]. Therefore, we believe that with better process control, much higher Q-factors are possible.

By repeated measurements of the same resonance dip, we have measured the system resolution, defined to be 3 times the standard deviation of peak position measurements [13], to be 78 pm. It should be noted here that the system resolution of 78 pm includes the effects of thermal fluctuation as well, since no temperature control was attempted during repeated measurements which lasted up to several minutes. However, the thermo-optic coefficient of SiN is of the order of  $10^{-5}$   $\text{K}^{-1}$ , which is more than 20 times lower than that of Si [19]. Furthermore, the slot structure by design concentrates a large fraction of the light in air. Thus, while the proposed structure requires temperature compensation for optimum performance as do most optical resonator sensors, the problem is expected to be less severe than comparable Si-based optical resonator sensors. Using this system resolution and the system sensitivity of  $2.5 \pm 0.2$  nm/( $\mu\text{g/ml}$ ) from Fig. 4 (b), we extrapolated a value of  $30 \pm 2$  ng/ml as the limit of detection for streptavidin. This value, with better fabrication process to obtain higher Q factors, can be lowered even further.

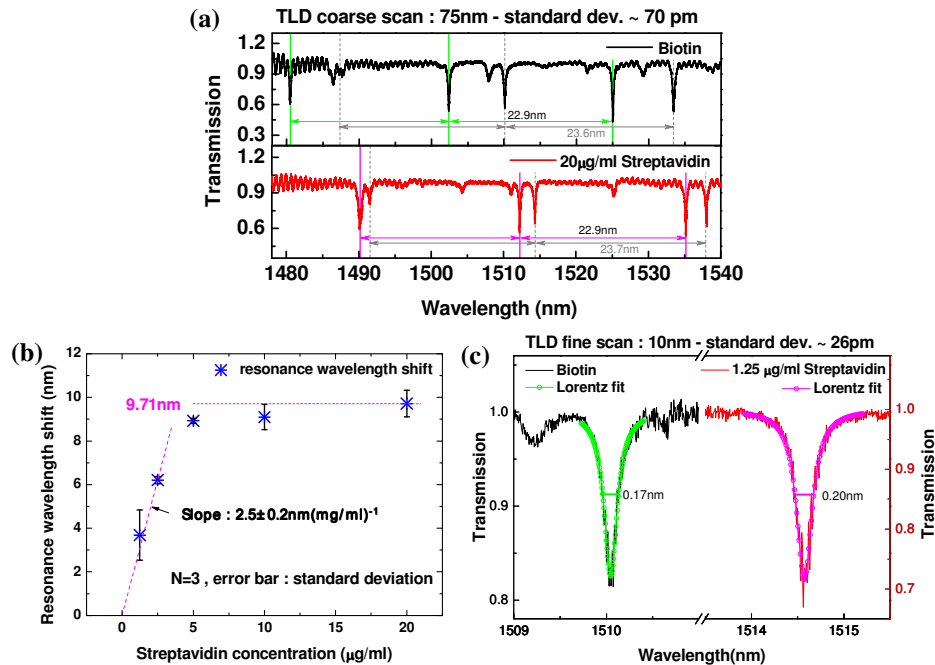


Fig. 4. (a) Transmission spectra before and after reacting streptavidin with concentration of 20 µg/ml (b) Dependence of the resonance peak shift of the fundamental radial mode on the streptavidin concentration. The initial linear slope gives the sensitivity, measured to be 2.48 nm/(µg/ml). (c) High resolution scan of the resonance dip before and after binding of streptavidin. The same Q-factor of ~7,000 is obtained in both cases.

#### 4. Conclusion

A SiN<sub>x</sub> horizontal air slot resonators with 15 µm diameter and 40nm wide air-slot was fabricated, and its bio-sensing ability was demonstrated. Using tapered fiber coupling, 6.2nm resonance wavelength shift upon reaction of biotin-streptavidin interaction was measured with concentration of 2.5 µg/ml. The surface sensitivity of streptavidin was obtained as  $2.5 \pm 0.2 \text{ nm}/(\mu\text{g/ml})$  assuming linear relationship. Comparing this value with surface sensitivity of 5.7 nm/nm calculated using FDTD simulations, a detection limit of  $30 \pm 2 \text{ ng/ml}$ , was extrapolated.

#### Acknowledgement

This work was supported in part by the Basic Science Research Program through NRF funded by MEST(2009-0087691), the Top Brand R&D program of MKE (09ZC1110: Basic Research for the Ubiquitous Lifecare Module Development). J. H. Shin acknowledges support by WCU (World Class University) program, grant No. (R31-2008-000-10071-0).